Journal of Inflammation Research

Dovepress
Taylor & Francis Group

Open Access Full Text Article

ORIGINAL RESEARCH

Study on the Mechanism of Artesunate in Modulating AR Epithelial Injury and Th2-Type Inflammatory Status

Youwei Bao*, Zhiqiang Zhang*, Binbin Shi, Qi Chen, Ying Zhang, Xinhua Zhu

Department of Otorhinolaryngology Head and Neck Surgery, The second Affiliated Hospital of Nanchang University, Jiangxi Medical College, Nanchang University, Nanchang, Jiangxi, 330006, People's Republic of China

*These authors contributed equally to this work

Correspondence: Xinhua Zhu, Department of Otorhinolaryngology Head and Neck Surgery, The second Affiliated Hospital of Nanchang University, Jiangxi Medical College, Nanchang University, Nanchang, Jiangxi, 330006, People's Republic of China, Email entzxh@126.com

Objective: To evaluate the therapeutic efficacy of Artesunate (ART) in a mouse model of allergic rhinitis (AR) induced by house dust mite (HDM) and explore its underlying mechanism.

Experimental Methods: Transcriptome sequencing (RNA-seq) analysis identified differentially expressed genes (DEGs) in nasal mucosa between healthy and allergic mice, with Gene Set Enrichment Analysis (GSEA) revealing STING pathway activation. We established a house dust mite (HDM)-induced allergic rhinitis (AR) mouse model via intraperitoneal sensitization. Artesunate (ART) efficacy was evaluated through dose-response testing (10–30 mg/kg), with 30 mg/kg identified as the optimal therapeutic dose. Mice were stratified into four groups: normal control (NC), NC+ART, AR model, and AR+ART-treated. Interventions were administered intraperitoneally, followed by systematic evaluation of: ① behavioral symptoms (sneezing/nasal scratching), ② histopathological changes in nasal and lung tissues, ③ serum TH2 cytokine levels, and ④ nasal mucosal protein expression profiles.

Results: With increasing concentrations of Artesunate (10, 20, 30 mg/kg), there was a significant improvement in the TH2 inflammatory status in AR mice. The cGAS-STING signaling pathway determines the degree of epithelial tissue inflammatory damage and systemic TH2-type inflammatory status in AR mice. Artesunate inhibits the cGAS-STING signaling pathway, protects the mitochondrial structure of epithelial tissue in AR mice, and improves epithelial damage and systemic TH2-type inflammatory status.

Conclusion: This study presents a new treatment approach for respiratory allergies by clarifying how Artesunate (ART) alleviates allergic rhinitis, identifying effective dosage ranges, and demonstrating its potential for developing ART- and cGAS-STING-targeted therapies, ultimately advancing clinical translation.

Keywords: allergic rhinitis, cGAS-STING, mitochondrial damage

Introduction

Allergic rhinitis, also known as hay fever, is a common nasal disorder characterized by inflammatory responses in the nasal mucosa. Its pathogenesis is complex, involving interactions among genetics, environment, and the immune system.[1–5] This disease is typically triggered by exposure to allergens such as pollen, dust mites, and animal dander, leading to a specific IgE antibody-mediated immune response. Consequently, symptoms such as nasal congestion, rhinorrhea, sneezing, and nasal itching arise, significantly impacting patients' quality of life.[6–12]

Inflammatory pathways in allergic rhinitis include the classical RAS-RAF-MAPK, JAK-STAT, and NF-κB signaling pathways. In recent years, increasing research has focused on the roles of the STING signaling pathway and NF-κB signaling pathway in allergic diseases.[9–11] The STING signaling pathway is a crucial DNA-sensing process that induces innate immunity against microorganisms and self-DNA damage. In allergic rhinitis, STING acts as an intracellular recognition receptor, capable of recognizing pathogenic DNA or self-DNA damage, thereby activating the cGAS-STING

Received: 15 January 2025
Accepted: 10 April 2025
Published: 18 April 2025

signaling pathway. Activation of this pathway induces the expression of interferons (IFNs) and other cytokines, which play vital roles in limiting viral replication and inducing cell apoptosis.[13–15] Recent studies have found that cGAS enhances lung fibroblast damage involving its own DNA. The cGAS / STING pathway reveals the sensing of cytoplasmic DNA as an activator of the immunoproteasome and CD8 + T cells. Furthermore, the STING pathway participates in the immune response process of allergic rhinitis by regulating the activation and function of immune cells.[11,16–20] Although the specific mechanisms are not fully understood, studies suggest that the STING pathway may be involved in regulating the Th1/Th2 immune balance, thereby influencing the occurrence and development of allergic rhinitis.[21,22]

The NF-κB signaling pathway regulates the expression of acute-phase reactant proteins, cytokines (such as TNF-α, IL-1, etc.), and cellular adhesion molecules. These inflammatory mediators play crucial roles in the inflammatory response of allergic rhinitis. Activation of the NF-κB signaling pathway may lead to overexpression of these mediators, thereby exacerbating the inflammatory response. Additionally, the NF-κB signaling pathway participates in the expression of immunoregulatory molecules, such as immunoregulatory factors and immune receptors. Changes in the expression of these molecules may affect the immune function of patients with allergic rhinitis, further influencing disease progression. NF-κB acts downstream of the STING signaling pathway, and their interactions can damage respiratory epithelial tissue, exacerbating epithelial barrier damage, allowing a large amount of allergens to enter the body, and triggering allergic reactions. Therefore, intervention in the STING/NF-κB axis represents a potential therapeutic direction for the treatment of allergic rhinitis.[13–15,21,22]

Recently, studies have found that artesunate, an antimalarial drug derived from the traditional Chinese medicine Artemisia annua, exhibits potential efficacy in the treatment of allergic respiratory diseases.[23–26] Artesunate possesses multiple mechanisms of action, including anti-inflammatory, anti-allergic, and immunoregulatory effects. It can inhibit mast cell degranulation and reduce the release of inflammatory mediators, thereby alleviating the symptoms of allergic rhinitis. Furthermore, artesunate may regulate the Th1/Th2 cell balance, correcting the overreaction of the immune system and further improving patients' allergic constitution.[27–31] Recent studies have found that artesunate regulates airway epithelial cell function and alleviates tissue damage function by inhibiting NLRP 3 inflammasome activation.[32–34]Although the exact mechanism of artesunate in the treatment of allergic rhinitis is not fully understood, it provides new therapeutic options and hope for patients with allergic rhinitis.[35–37]

In this study, we constructed an AR mouse model and used artesunate (ART) as an intervention to observe pathological changes in the nasal mucosa, bronchi, and lung tissue of the mice, as well as the expression of airway tissue proteins and Th2 cytokines in the serum. Additionally, we focused on the inflammatory state and airway remodeling in the nasal mucosa, bronchi, and lung tissue. The aim of this study was to investigate the role and significance of cGAS-STING in the AR mouse model, providing new insights and experimental evidence for future respiratory health and cGAS-STING drug development. In this study, we used artesunate (ART) at various concentrations (10, 20, 30 mg/kg) to explore the effective dose.[30,31,37] However, this experiment was the first to explore its efficacy in treating the AR mouse model. Notably, the stability of the ART treatment effect in this experiment was not ideal, which may have affected the consistency of the treatment outcome. Despite this, the study conducted preliminary and meaningful explorations in animal experiments, providing crucial evidence for understanding the role of artesunate in the treatment of respiratory allergic diseases by improving the STING signaling pathway.

Materials and Methods

Transcriptome Sequencing Analysis

Transcriptome RNA sequencing was performed by Shanghai OE Biotech Co., Ltd. (Shanghai, China). Nasal mucosa tissues were collected from OVA-induced mice for transcriptome analysis. Genes with $|\log2(\text{fold change, Fc})| > 1$ and a significant p-value < 0.05 assessed by DESeq2 were classified as differentially expressed genes (DEGs) between the two groups. The intersection of DEGs from both groups was obtained. Functional annotation of DEGs was conducted using the Database for Annotation, Visualization, and Integrated Discovery (DAVID) (https://david.ncifcrf.gov/) for Gene Ontology (GO) and Kyoto Encyclopedia of Genes and Genomes (KEGG) pathway enrichment analysis, including

biological process (BP), cellular component (CC), and molecular function (MF). GO and KEGG terms with $p < 0.05$ were considered significantly enriched by DEGs.

Animals and Treatment Protocols

Female Balb/c mice aged 6 to 8 weeks were provided by the Animal Science Department of Nanchang University Medical College. The mice were housed in specific pathogen-free conditions at the Animal Center of Jiangxi Medical College, Nanchang University. The entire experimental protocol was approved by the Institutional Animal Care and Use Committee of the Jiangxi Medical College, Nanchang University Ethics Committee, Approval Nos. NCULAE-202210311028, and in line with the Global Strategies for the Ethical Treatment and Utilization of Laboratory Animals.

The mice were divided into the following groups: ① Normal Control (NC), ② AR, ③ AR+ART10, ④ AR+ART20, ⑤ AR+ART30, and ⑥ AR+DXMS. Each group consisted of 6 female Balb/C mice aged 6–8 weeks. Mice in the AR group were sensitized by intraperitoneal injection of 200ul of sensitizing solution on days 0, 7, and 14. From days 21 to 27, they received 20ul of nasal challenge solution intranasally once a day. Mice in the NC group underwent the same procedures but with an equal volume of PBS instead of the sensitizing and challenge solutions. All mice were euthanized and tissues were collected on day 28.

The sensitizing solution was prepared by dissolving HDM powder in PBS to a concentration of 1mg/mL. An appropriate amount was mixed with a 10-fold diluted aluminum hydroxide suspension in a 1:1 volume ratio. Each mouse received 200ul of the sensitizing solution intraperitoneally each time. The nasal challenge solution was prepared by dissolving HDM in PBS, with each 20μL of PBS containing 20ug of HDM. Artesunate (ART, MCE, HY-N0193) was administered intraperitoneally at doses of 10/20/30mg/kg for 7 consecutive days, 30 minutes before each nasal challenge. Dexamethasone (DXMS) was administered intraperitoneally at a dose of 2mg/kg. The mice were anesthetized with isoflurane (1–5%) to induce and maintain anesthesia for 24 hours before euthanasia and tissue collection (Figure 1A).

Nasal Symptom Scoring

Each group of mice recorded symptoms, sneezing and scratching times within 10 min on day 28, after the last nasal stimulation.

Histological Studies

For histological analysis, the heads of the mice were removed, and the nasal septum was completely dissected. The nasal mucosa was scraped using a hooked tweezer and placed in an EP tube containing 10% neutral formalin for pathological section staining. The lungs were removed and fixed in 4% paraformaldehyde solution for 24 hours. The fixed nasal and lung tissues were embedded in paraffin, and 4mm-thick tissue sections were mounted on slides, dewaxed, and stained with hematoxylin and eosin (HE) and Masson's trichrome. The pathological changes in the nasal and lung tissues were analyzed under a light microscope (Thermo Fisher Scientific, USA) at 400X magnification.

HE staining was used to assess inflammation in the nasal and lung tissues. The degree of inflammatory cell infiltration around the microairways was used to quantify the level of inflammation, with scores ranging from 0 to 4. The criteria were: 0, no cells; 1, a few inflammatory cells infiltrating around the airways; 2, 1–2 layers of inflammatory cell infiltration; 3, 3–5 layers of infiltration; 4, more than 5 layers of infiltration.

Masson's trichrome staining was used to assess the deposition of collagen fibers in the airways, which were stained blue. The percentage of collagen fiber area was calculated using Image J software by measuring the blue-stained area.

Immunohistochemical Analysis

Immunohistochemistry was used to determine the location and concentration of STING protein. Lung paraffin sections were dewaxed and rehydrated, then treated with 3% hydrogen peroxide. The sections were then blocked with 5% goat serum to reduce interference from nonspecific immunoglobulins. The specimens were incubated with anti-STING antibody (proteintech, 66680-1-Ig, 1:500) at 37°C for 2 hours, followed by incubation with secondary antibody at 37°C for 30 minutes. Image-J software was used to assess protein expression. Observations were made at 400X magnification.

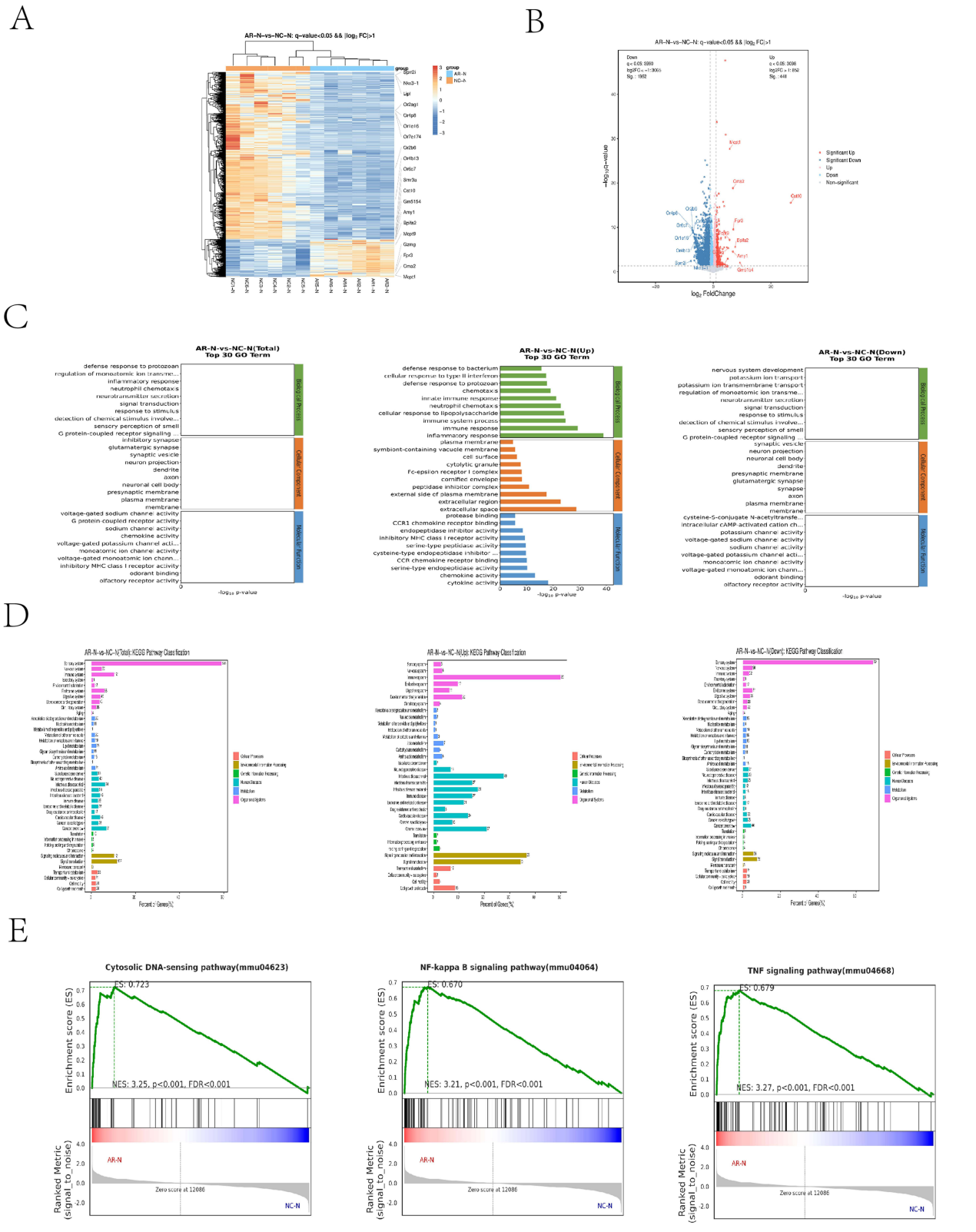

Figure 1 Transcriptional analysis of nasal mucosa tissue from normal group and allergic rhinitis group mice using RNA-seq technology.(**A** and **B**) Differentially expressed genes (DEGs) from allergic group and normal group, volcano plot. Normal vs allergic rhinitis mice, based on the RNA-seq results.(**C** and **D**) Venn diagram of up-regulated and downregulation of GEGs.(**E**) Analysis of DEGs between normal vs allergic rhinitis groups using GSEA for cytosolic DNA, NFKB, TNF pathway.

Measurement of IL-4, IL-5, IL-13, and IgE Levels in Serum

Levels of IL-4(meimian, MM-0165M1), IL-5(meimian, MM-0164M1), IL-13(meimian, MM-0173M1) and IgE(meimian, MM-0056M1) in serum were determined using ELISA kits (Wuhan Experimental Technology Co., Ltd., China) according to the manufacturer's instructions. All procedures were strictly conducted in accordance with the ELISA kit manual.

Western Blotting

Proteins were extracted from lung tissues using RIPA lysis buffer containing protease inhibitor (GRF101, Epizyme) and phosphatase inhibitor cocktails (GRF102, Epizyme), and quantified using a BCA protein assay kit (ZJ101, Epizyme). Equal amounts of protein were subjected to electrophoresis on polyacrylamide gels and transferred to polyvinylidene fluoride (PVDF) membranes. Primary antibodies, including those for actin(proteintech, 60008-1-Ig, 1:5000), cGAS (proteintech, 68640-1-Ig, 1:1000), sting(proteintech, 66680-1-Ig, 1:5000), P-NF-KB(CST, 3033T, 1:1000), NF-KB (CST, 8242T, 1:1000), were incubated with the membranes for 2 hours at room temperature. After incubation with secondary antibodies for 40 minutes at room temperature, the membranes were detected using a chemiluminescent substrate system (Bio-Rad Laboratories, CA, USA). The band intensities of proteins were quantitatively analyzed using Image J software.

Electron Microscopy

Tissue samples (approximately 1 mm^3 in size) or collected cells (approximately 10^7 cells) were immediately fixed in 2.5% glutaraldehyde for 24 hours. The fixative was then replaced with PBS buffer for 6 hours, followed by postfixation in 1% osmium acid for 2 hours. Specimens were dehydrated in a graded series of ethanol concentrations (from 30% to 100%) and propylene oxide, infiltrated with a mixture of propylene oxide and epoxy resin, and finally embedded in pure epoxy resin. The embedded tissues were sectioned and scanned using an electron microscope.

Data Analysis

Data are presented as mean ± standard deviation (SD). All analyses were performed using GraphPad Prism 6.0 software. Normality test: All continuous variables (such as cytokine level, protein expression level) were confirmed to meet the normal distribution ($p > 0.05$), meeting the requirements of ANOVA application. Independent sample *t*-tests and one-way ANOVA were conducted for comparisons between two groups and multiple groups, respectively. Post hoc tests included Tukey's HSD test for homogeneity of variances or Dunnett's T3 test for heterogeneity of variances.

Results

Transcriptome Analysis

To analyze the differences in transcriptome levels of nasal mucosa tissues in house dust mite (HDM)-induced allergic rhinitis (AR) mice at the molecular level, transcriptome sequencing was employed to identify differentially expressed genes (DEGs) between the control group and the AR group. Based on the screening criterion of $|\log2(\text{fold change, Fc})| > 1$ and a significant p-value < 0.05 (compared to the control group), 2393 genes exhibited significant changes in the AR group, with 441 genes upregulated and 1952 genes downregulated. A volcano plot was used to visualize the upregulation and down-regulation of genes in the normal control (NC) and AR groups.

To further investigate the differential molecules associated with AR and identify key molecules, GO enrichment and KEGG signaling pathway analyses were conducted on the DEGs in the nasal mucosa tissues of AR and NC groups. Compared to the NC group, the most significantly upregulated GO terms in the AR group were "inflammatory response", "extracellular region", and "cytokine activity". The top 20 pathways, based on a p-value < 0.05, were considered primary pathways. The results indicated that the main KEGG pathways in AR compared to NC included Sensory system, Signal transduction, Immune system, Signaling molecules and interaction, and Cancer: overview. The most enriched gene pathway was the Sensory system pathway, with 696 genes involved (Figure 1A–C).

To further validate the differences observed in the transcriptome analysis between the two groups, Gene Set Enrichment Analysis (GSEA) was employed. This method determines whether a predefined set of genes shows a

statistically significant, consistent difference between two groups. GSEA results revealed that the cytosolic DNA sensing pathway (mmu04623), NF-kappa B signaling pathway (mmu04064), and TNF signaling pathway (mmu04668) were significantly enriched in the AR group. These three pathways are related to the STING signaling pathway and are mediated by inflammatory damage in the allergic state. Mitochondrial damage leads to the leakage of mtDNA into the cytosol, activating STING, which subsequently activates the NF-κB and TNF signaling pathways (Figure 1D and E).

Artesunate Improves Behavioral Status

After the final nasal challenge, the number of sneezes and nasal scratching behaviors within 10 minutes were recorded and quantified for scoring in mice. The artesunate (ART) intervention group exhibited a significantly higher number of sneezes and nasal scratching compared to the normal control group, but these behaviors were mitigated compared to AR mice, with statistically significant differences. However, both the ART intervention group and the AR group had higher scores than the normal control group. Behavioral observations and analyses of mice indicated that the application of ART in the interference model effectively controlled nasal symptoms in AR mice (Figure 2A and B).

Improvement of AR Inflammatory Status by Artesunate at Different Concentrations

The levels of IL-4, IL-5, IL-13, and IgE were summarized in a table after being quantified through ELISA. The differences marked with NS (not significant) had no statistical significance. All other comparisons among the NC group, AR group, AR+ART10 group, AR+ART20 group, AR+ART30 group, and AR+DXMS group showed statistically significant differences. As the concentration of artesunate (ART) increased, TH2-type inflammatory cytokines were significantly improved.

Specifically, the levels of IL-4, IL-5, and IL-13, which are key cytokines involved in the TH2-mediated immune response and are associated with allergic inflammation, were reduced in a concentration-dependent manner in the ART-treated groups compared to the AR group. Similarly, the level of IgE, a key mediator of allergic reactions, was also decreased with increasing concentrations of ART. These findings suggest that artesunate has a therapeutic effect on AR by inhibiting TH2-type inflammatory responses and reducing the production of allergic mediators (Figure 2C).

Overall, the results demonstrate that artesunate can effectively improve the inflammatory status of AR in a concentration-dependent manner, providing a potential therapeutic option for the treatment of allergic rhinitis.

Improvement of Mitochondrial Damage in AR Epithelial Tissue by Artesunate (Electron Microscopy and Western Blotting)

Observation of Nasal Mucosa Epithelial Cells by Electron Microscopy

Mitochondria serve as the "energy factories" within cells, responsible for generating ATP (adenosine triphosphate) to provide energy for cellular functions. In the inflammatory state of allergic rhinitis (AR), immune cells are activated and release a large amount of inflammatory mediators and cytokines. These mediators and cytokines can induce oxidative stress, leading to the production of excessive reactive oxygen species (ROS) and reactive nitrogen species (RNS) within mitochondria. Oxidative stress damages mitochondrial DNA, proteins, and lipids, affecting the normal function of mitochondria. It disrupts mitochondrial membrane potential, resulting in mitochondrial dysfunction, including impaired respiratory chain, reduced ATP synthesis, and increased mitochondrial membrane permeability (Figure 3A).

We observed the state of mitochondria in nasal mucosa epithelial cells under electron microscopy. The results showed that in the AR group, the organelles were disorganized and swollen, with some mitochondria becoming swollen and rounded, and their cristae disappearing. However, in the ART group (30 mg/kg), mitochondrial structure was improved, with less swelling compared to the AR group.

Western Blotting Detection of Mitochondrial Protein Levels

PGC-1α and TFAM are essential for maintaining normal mitochondrial function and cellular health by regulating mitochondrial DNA replication and transcription, promoting mitochondrial biosynthesis, enhancing resistance to oxidative stress, and modulating inflammatory responses. Western blotting was used to detect the levels of mitochondrial proteins PGC-1α and TFAM. Compared to the NC group, the levels of these mitochondrial proteins were significantly

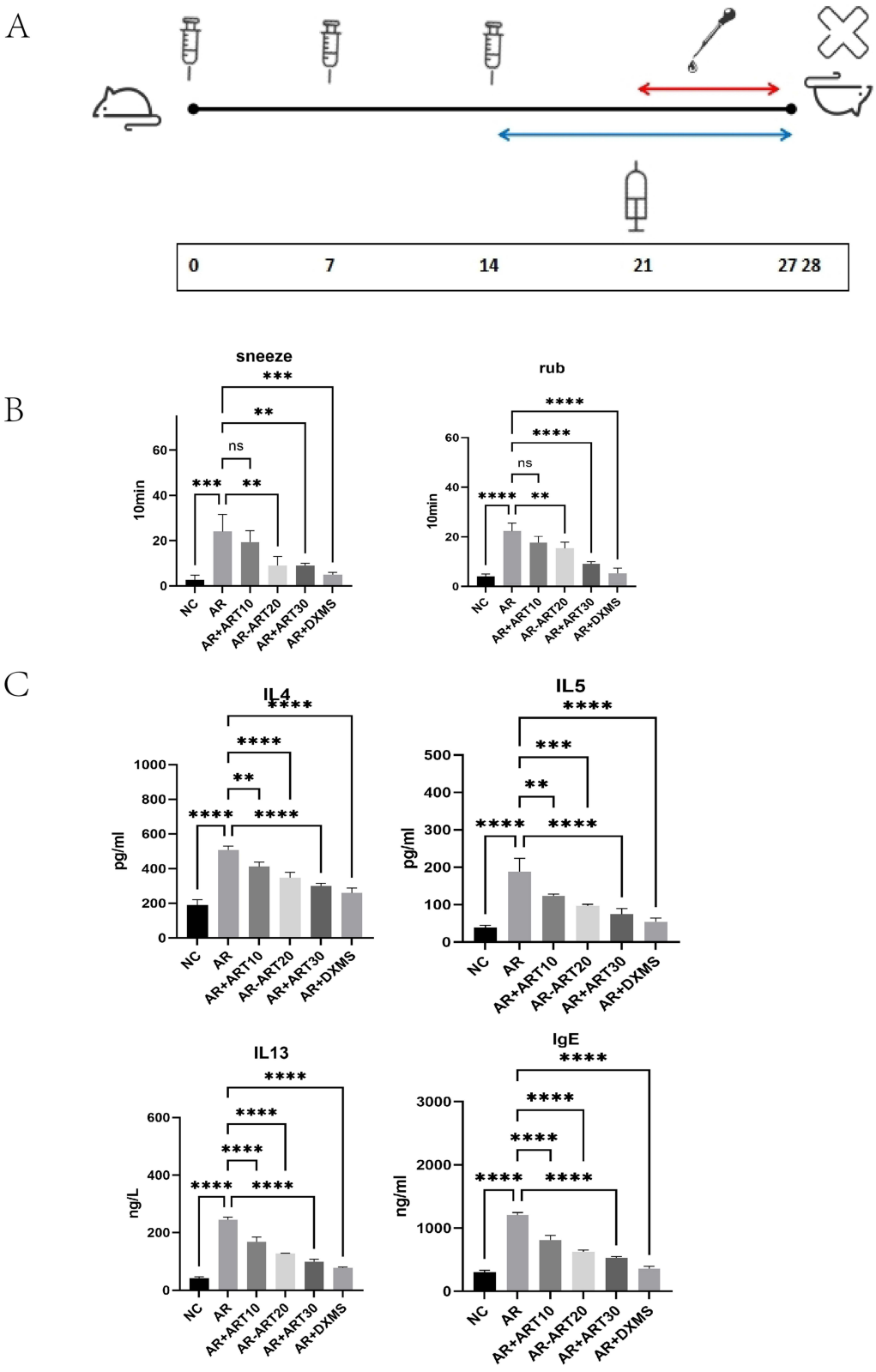

Figure 2 Gradient concentration administration: (**A**) Flow chart of the HDM molding AR model; (**B**) Sneezing count after nasal challenge in mice; Scratching nose count after nasal challenge in mice.(**C**) The levels of IL-4, IL 5, IL-13, and Ige were determined by ELISA. **P < 0.01, ***P < 0.001,****P<0.0001. Results were analyzed using one-way and two-way analysis of variance followed by Tukey's post-hoc test. The results are presented as mean ± standard deviation.

https://doi.org/10.2147/JIR.S513760

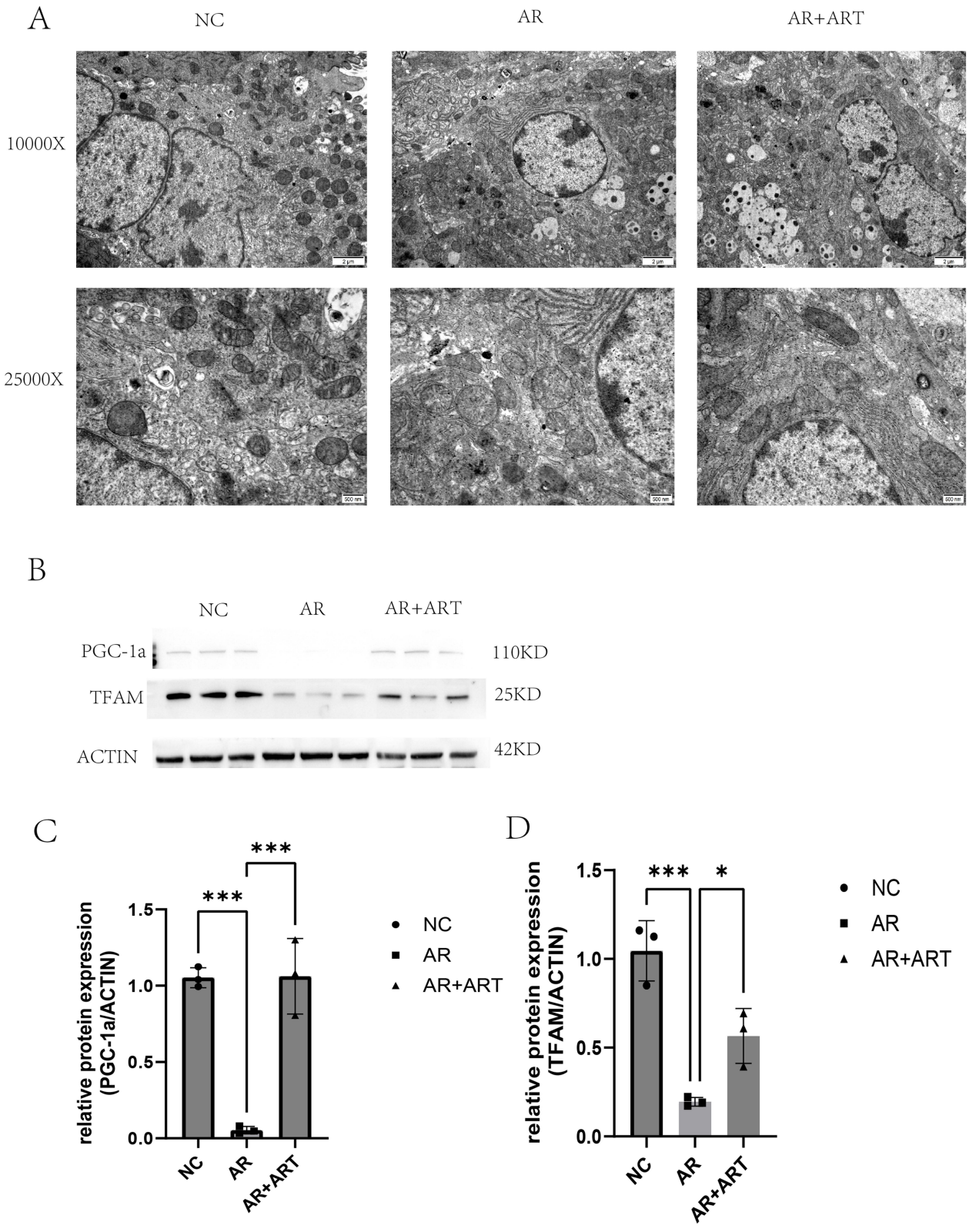

Figure 3 Mitochondrial status of the nasal mucosal epithelial tissue after intervention with ART (default 30 mg / kg).(**A**) For EM observation of the epithelial tissue of the nasal mucosa (10000X, 25000X); (**B**) PGC-1a, TFAM expression measured by WB; (**C** and **D**). Statistics were obtained between PGC-1a, TFAM and actin. *P < 0.05, ***P < 0.001.Results were analyzed using one-way and two-way analysis of variance followed by Tukey's post-hoc test. The results are presented as mean ± standard deviation.

reduced in the AR group. However, after ART intervention, PGC-1α and TFAM levels increased. At the protein level, mitochondria in the AR state exhibited damage to normal mitochondrial proteins, while ART reversed this damage and promoted mitochondrial biogenesis.

Overall, these findings suggest that artesunate can improve mitochondrial damage in AR epithelial tissue by protecting mitochondrial structure and function, potentially through reducing oxidative stress and enhancing mitochondrial biogenesis. This provides further evidence for the therapeutic potential of artesunate in the treatment of allergic rhinitis (Figure 3B–D).

Artesunate Inhibits the cGAS-STING Signaling Pathway to Alleviate Epithelial Damage and Systemic TH2 Inflammatory Status in AR

Behavioral Change

The last nasal challenge of mice, the number of sneezes and nasal scratching within 10 minute were recorded, and the processing data were quantified. The number of nasal grasping and sneezing was significantly higher in the AR + ART group than in the AR group, and the difference was statistically significant. The above behavioral observations and analysis of mice showed that ART interference can effectively control the nasal symptoms of AR mice (Figure 4A).

HE Staining Results

Observations of the nasal mucosa tissue of mice showed that combined ART intervention in AR mice inhibited nasal mucosa inflammation, reducing the infiltration of inflammatory cells and promoting a certain degree of recovery of the mucosa and its surface cilia (Figure 2). Examination of the lung tissue of the four groups of mice revealed that alveolar tissue, inflammatory infiltration, and interstitial inflammation were all reduced in the ART group compared to the AR group. The successful establishment of the AR model also caused inflammation-related changes in the nasal mucosa and lung tissue, demonstrating the mutual influence between allergic rhinitis and asthma. After the use of ART in AR mice, the inflammatory state of the lungs improved significantly, proving that the STING signaling pathway has a pro-inflammatory effect on allergic lung diseases (Figure 4B and C).

Masson Staining

To explore the effect of ART intervention on airway remodeling in the nasal cavity and lung tissue of mice, this experiment used Masson staining to observe and compare the distribution of collagen fibers in the nasal and lung tissues of mice in each group. The sections were observed under a high-power microscope (400×). First, the nasal mucosa was observed, and it was found that the collagen fibers in the submucosa of the AR group were widely distributed and stained significantly, consistent with allergic rhinitis. In the AR+ART group, the content of collagen fibers in the submucosa was lower than that in the AR group, and the distribution range was reduced. After ART treatment, there was a protective effect on the lung structure of the AR group, with a significant reduction in inflammatory cells and edema in the lung tissue, as well as a reduction in the number and severity of alveolar ruptures. Although there was still a small amount of inflammatory cell infiltration, it was significantly reduced compared to the AR group (Figure 4B and C).

Immunohistochemical Results

To investigate the effect of ART intervention on the infiltration of inflammatory cells in the nasal mucosa and lungs of mice, STING monoclonal antibodies were used, which are highly expressed in the cytoplasm of respiratory epithelial cells. After staining, the sections were observed under a high-power microscope (400×).

In the nasal mucosa, we found that the allergic group had significant inflammatory infiltration and mucosal damage. In the antibody-treated group, mucosal damage and inflammatory cell infiltration were less severe than in the allergic rhinitis group, and there was no significant difference in the specific therapeutic effect between the two antibodies. The combination of the two antibodies had the best effect. In bronchial sections, significant inflammatory infiltration and bronchial damage were found in the allergic group. The NC group showed no obvious abnormalities in the lung field; the AR group showed obvious structural disorders in the lung field, with no obvious normal tissue, interstitial edema, and structural damage; in the ART group, lung inflammation, edema of lung tissue, and alveolar structure were significantly improved compared to the AR group, with only a small amount of inflammatory cell infiltration observed in the lung tissue compared to the AR group (Figure 4B and C).

https://doi.org/10.2147/JIR.S513760

ELISA Detection of Serum Levels of Related Inflammatory Mediators and Cytokines (IL-4, IL-5, IL-13, IgE)

The levels of IL-4, IL-5, IL-13, and IgE, as determined by ELISA, are summarized in the table The differences marked with NS were not statistically significant. The differences between the NC group, NC+ART group, AR+ART group, and the allergic rhinitis (AR) group were statistically significant. We found that the use of ART reduced the levels of TH2 inflammatory cytokines in mice with allergic rhinitis, thereby alleviating the TH2 cell imbalance in respiratory allergic diseases (Figure 4D).

WB Detection of Protein Levels in Nasal Mucosa Tissue

When the epithelial barrier is damaged, it triggers intracellular DNA sensing mechanisms, including the activation of the cGAS-STING pathway. This activation may further exacerbate epithelial cell damage and inflammation, thereby

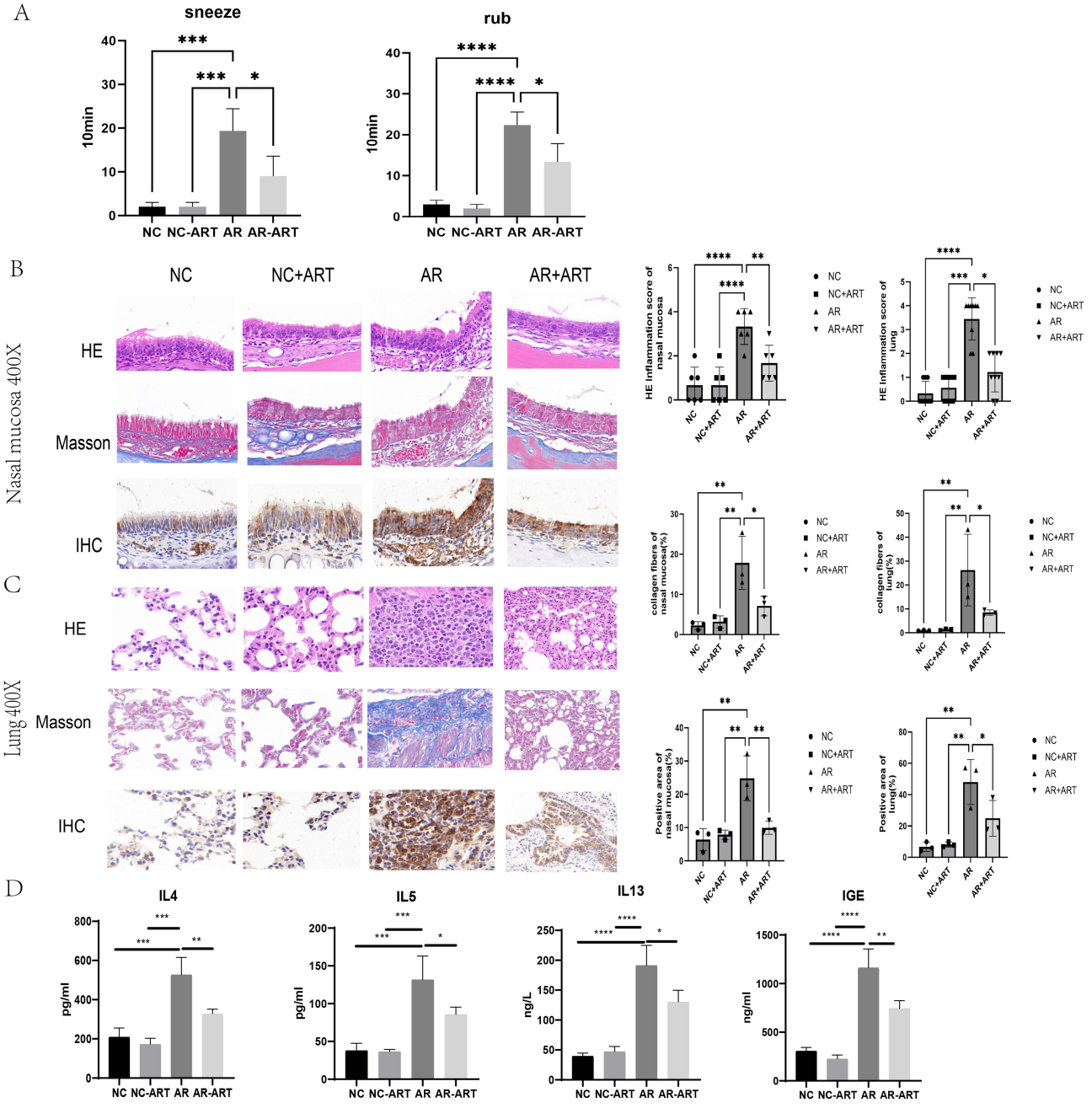

Figure 4 Continued.

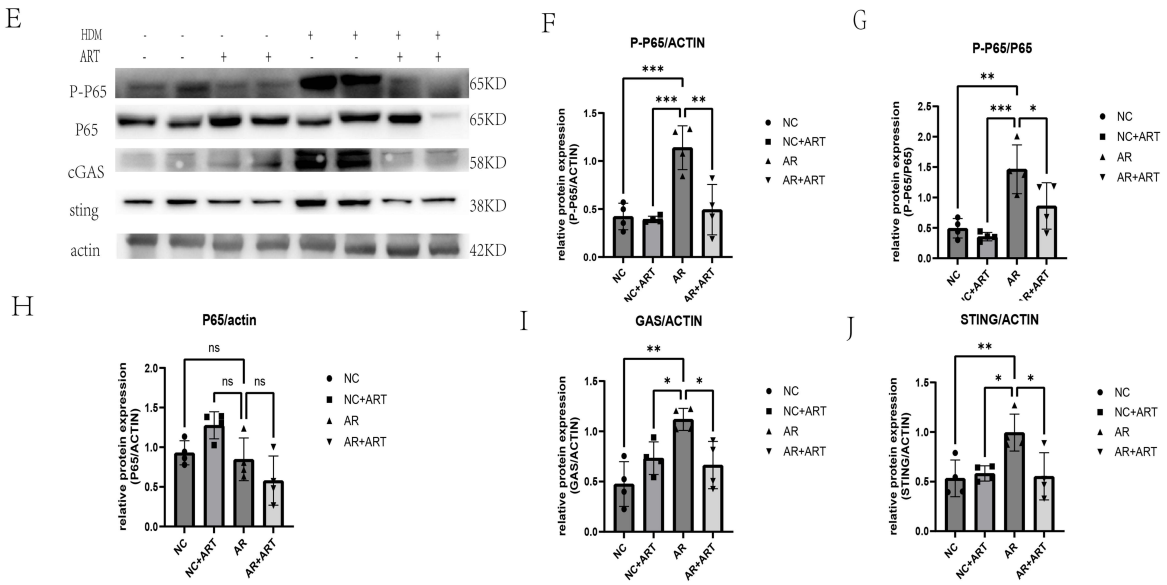

Figure 4 ART (30 mg / kg) intervention mice were used to detect the stings pathway expression level and TH 2 inflammation level in the nasal mucosa of each group.(**A**) Mice symptom data; (**B**) HE, MASSON, pathological section images and data statistics of nasal mucosa and lung tissue of IHC; (**C** and **D**) After ART, TH 2 inflammatory factors in each group: IL-4, IL-5 IL-13, Ige; (**E**) Expression levels of the sting signaling pathway: cGAS, STING, P-NF-KB, NF-KB.(**F–J**) Statistics were obtained between cGAS, STING, P-NF-KB, NF-KB and actin. *P < 0.05, **P < 0.01, ***P < 0.001,****P<0.0001. Results were analyzed using one-way and two-way analysis of variance followed by Tukey's post-hoc test. The results are presented as mean ± standard deviation.

worsening the symptoms of allergic rhinitis. STING can also activate IKK, leading to the phosphorylation of NF-κB. Phosphorylated NF-κB then enters the nucleus and induces the expression of related cytokines. The activation of NF-κB can also affect the activity of the STING pathway. For example, the NF-κB signaling pathway can prevent the degradation of STING by altering microtubule-mediated STING trafficking, thereby prolonging and enhancing the STING-mediated immune response. We detected the levels of cGAS, STING, and NF-κB in nasal mucosa epithelial tissue. After stimulation with house dust mites (HDM), the levels of cGAS, STING, and phosphorylated NF-κB (P-NF-κB) increased. After intervention with ART (30 kg/mg), the levels of cGAS, STING, and P-NF-κB in the allergic epithelial tissue were effectively reduced (Figure 4E–J).

Discussion

Allergic rhinitis (AR) leads to damage to the nasal mucosal epithelial cells. The interaction between allergens and nasal mucosal epithelial cells, followed by the subsequent inflammatory response, can cause damage and dysfunction to the epithelial cells. When the epithelial cells are damaged, their barrier function is compromised, allowing more allergens and inflammatory mediators to enter the submucosa, further exacerbating the inflammatory response and damage. Additionally, the damage to epithelial cells may impair their normal physiological functions, such as mucus secretion and ciliary motion, thereby affecting the nasal cavity's cleansing and defensive functions. In AR, the damage and repair process of epithelial cells may be in a dynamic balance. Continuous inflammatory responses and allergen stimulation may lead to persistent damage and poor repair of epithelial cells, forming a vicious cycle that exacerbates disease progression.

Transcriptome analysis of nasal mucosal epithelia revealed significant increases in the transcriptome of circular DNA, NF-κB, and TNF-α signaling pathways in the AR group compared to the NC group. Normally, DNA originates from the nucleus and mitochondrial structures, with nuclear DNA enclosed by the nuclear membrane and not leaking into the cytoplasm. However, under conditions such as cell damage, inflammation, or viral infection, mitochondrial mtDNA may leak into the cytoplasm and become cytosolic DNA. The cGAS-STING signaling pathway then activates the downstream NF-κB signaling pathway, further leading to the release of TNF-α from epithelial inflammatory damage.

In this study, artesunate (ART) demonstrated a protective effect on epithelial tissue during the treatment of AR, with a specific effective concentration of 30 kg/mg determined. ART improves epithelial damage in AR mouse models primarily

 https://doi.org/10.2147/JIR.S513760

by inhibiting the cGAS-STING signaling pathway in respiratory epithelial tissue, protecting against abnormal activation and damage to epithelial tissue. Overactivation of the cGAS-STING signaling pathway exacerbates the inflammatory state of epithelial tissue, while ART intervention mitigates this damage, preserving the integrity of epithelial tissue and reducing the opportunity for allergens to enter the body. IgE is an immunoglobulin that plays a crucial role in allergic diseases such as AR. ART alleviates allergic symptoms by regulating the immune system and inhibiting IgE release. Furthermore, ART reduces the levels of TH2-type inflammatory cytokines in the serum, such as IL-4, IL-5, and IL-13, which are key players in type 2 inflammatory responses. By inhibiting the release of these inflammatory cytokines, ART attenuates the inflammatory response in AR and improves the allergic state.

Mitochondria are the "energy factories" within cells, responsible for producing ATP and providing energy to the cell. Nasal mucosal epithelial cells in patients with allergic rhinitis are often subjected to inflammatory attacks, leading to epithelial damage. This damage may manifest as epithelial cell shedding, increased cell gaps, and thickening of the basement membrane. Epithelial damage not only disrupts the barrier function of the nasal mucosa but may also trigger or exacerbate inflammatory responses. Oxidative stress is one of the important factors leading to mitochondrial damage. In allergic rhinitis, allergens and inflammatory mediators may stimulate cells to produce excessive reactive oxygen species (ROS), thereby damaging mitochondria. Damaged mitochondria may produce more ROS, forming a vicious cycle that exacerbates epithelial cell damage. Additionally, mitochondrial damage may lead to insufficient energy supply, affecting the repair and regeneration capabilities of epithelial cells. The repair and regeneration of epithelial cells are crucial for maintaining the barrier function of the nasal mucosa. Promoting the functional recovery of mitochondria, improving cellular energy supply, and enhancing repair capabilities through drugs or other means are potential therapeutic strategies for improving mitochondrial damage. In this study, electron microscopy observations of epithelial cell mitochondria showed that compared to the NC group, mice in the AR group had swollen mitochondria in nasal mucosal tissue epithelia, with content leakage and altered cristae structures. The mitochondrial-related proteins PGC-1α and TFAM were detected. The results showed that AR damaged normal mitochondrial proteins PGC-1α and TFAM, and the use of ART at 30 mg/kg could reverse mitochondrial damage. In terms of mitochondrial structure, ART improved the mitochondrial envelope structure, reduced swelling, restored the inner cristae structure, and decreased the outflow of contents. At the level of mitochondrial structural proteins, PGC-1α and TFAM increased compared to AR. PGC-1α and TFAM are mitochondrial biogenesis proteins, and their levels represent the level of mitochondrial proliferation and division. Therefore, the use of ART improved OVA-induced mitochondrial damage.

Pathological sections were used to observe the nasal mucosa and lung tissue, with HE, Masson, and IHC (STING) staining employed to assess the damage state of epithelial tissue. Observations of mouse nasal mucosal tissue showed that combined ART intervention inhibited nasal mucosal inflammation in AR mice, reducing the infiltration of inflammatory cells and restoring the mucosa and its surface cilia to some degree. In lung tissue, the alveolar tissue, inflammatory infiltration, and interstitial inflammation were all reduced in the ART group compared to the AR group. The successful establishment of the AR model also resulted in inflammatory-related changes in the nasal mucosa and lung tissue, demonstrating the interaction between allergic rhinitis and asthma. After using IHC, STING protein was highly expressed in the respiratory epithelial tissue of AR mice, both in nasal mucosal tissue and lung epithelial tissue. These results were consistent with those of HE and Masson staining.

Finally, we used ELISA to detect TH2 cytokines (IL-4, IL-5, IL-13, IgE) and WB to detect the STING and NF-κB pathways. The use of ART (30 kg/mg) improved the TH2-type inflammatory state in mice and inhibited both the STING and NF-κB pathways after intervention. The STING signaling pathway plays a pivotal role in the damage to the inflammatory state of epithelial tissue in AR mice. Excessive activation of the STING signaling pathway may exacerbate respiratory allergic symptoms, such as airway inflammation and airway hyperreactivity. In the AR mouse model, the STING signaling pathway was activated, leading to epithelial tissue damage. Artesunate inhibits the STING signaling pathway, thereby protecting the mitochondrial structure of epithelial tissue in AR mice and improving epithelial damage. NF-κB is a downstream pathway of the STING signaling pathway and is also a classic inflammatory signaling pathway that is upregulated in the AR mouse model, participating in the inflammatory damage to epithelial tissue. By inhibiting the NF-κB signaling pathway, the inflammatory response in respiratory epithelial tissue can be reduced, thereby improving epithelial damage. In this study, the use of artesunate reduced the STING pathway in AR mouse tissues and inhibited NF-κB protein levels. This provides a specific therapeutic mechanism for artesunate in the treatment of allergic rhinitis and even respiratory allergic diseases.

However, the limitation of this experiment are the focus on mechanism exploration in mouse model and lack of clinical experiments and in vitro cell experiments. In addition, the mechanism verification part should deepen the ROS detection and mitochondrial DNA leakage quantification experiments to judge the state of mitochondrial damage. This study provides a mechanism basis for ART in AR, but its clinical transformation needs further verification, including human safety assessment, dose optimization and long-term efficacy tracking.

Conclusion

This study confirmed the effect of ART in treating allergic rhinitis in mice and revealed that ART can inhibit the expression of sting and NF-KB protein to inhibit nasal mucosa and lung epithelial damage and reduce systemic Th type 2 inflammatory cytokine release in mice. This study provides a mechanism basis for ART in AR, but its clinical transformation needs further verification, including human safety assessment, dose optimization and long-term efficacy tracking.

Author Contributions

All authors made a significant contribution to the work reported, whether that is in the conception, study design, execution, acquisition of data, analysis and interpretation, or in all these areas; took part in drafting, revising or critically reviewing the article; gave final approval of the version to be published; have agreed on the journal to which the article has been submitted; and agree to be accountable for all aspects of the work.

Funding

This research was supported by a grant (82060186) from the National Natural Science Foundation of China and a grant (20224ACB206025; 20232BAB216058) from Natural Science Foundation of Jiangxi Province. The Jiangxi Provincial Graduate Student Innovation Program(YC2024-B070).

Disclosure

The authors declare no competing interests in this work.

References

1. Bernstein JA, Bernstein JS, Makol R, et al. Allergic rhinitis: a review. *JAMA-J Am Med Assoc*. 2024;331(10):866–877. doi:10.1001/jama.2024.0530
2. Bousquet J, Anto JM, Bachert C, et al. Allergic rhinitis. *Nat Rev Dis Primers*. 2020;6(1):95. doi:10.1038/s41572-020-00227-0
3. Cox LS. Sublingual immunotherapy for allergic rhinitis: is 2-year treatment sufficient for long-term benefit? *JAMA-J Am Med Assoc*. 2017;317(6):591–593. doi:10.1001/jama.2017.0128
4. Dutra Silva J, Su Y, Calfee CS, et al. Mesenchymal stromal cell extracellular vesicles rescue mitochondrial dysfunction and improve barrier integrity in clinically relevant models of ARDS. *Eur respir j*. 2021;58(1):null. doi:10.1183/13993003.02978-2020
5. Kodera Y, Chiba H, Konno T, et al. HMGB1-downregulated angulin-1/LSR induces epithelial barrier disruption via claudin-2 and cellular metabolism via AMPK in airway epithelial Calu-3 cells. *Biochem Biophys Res Commun*. 2020;527(2):553–560. doi:10.1016/j.bbrc.2020.04.113
6. Nikolis A, Avelar LET, Haddad A, et al. Turn your AART into a HIT using a complete range of aesthetic injectables: methodology for combining products to maximise patient outcomes. *Clin Cosmet Invest Dermatol*. 2024;17(null):2051–2069. doi:10.2147/CCID.S465155
7. Ordovas-Montanes J, Dwyer DF, Nyquist SK, et al. Allergic inflammatory memory in human respiratory epithelial progenitor cells. *Nature*. 2018;560(7720):649–654. doi:10.1038/s41586-018-0449-8
8. Rangarajan S, Bernard K, Thannickal VJ. Mitochondrial dysfunction in pulmonary fibrosis. *Ann Am Thorac Soc*. 2017;14(Supple5):S383–s8. doi:10.1513/AnnalsATS.201705-370AW
9. Scadding GW, Calderon MA, Shamji MH, et al. Effect of 2 years of treatment with sublingual grass pollen immunotherapy on nasal response to allergen challenge at 3 years among patients with moderate to severe seasonal allergic rhinitis: the grass randomized clinical trial. *JAMA-J Am Med Assoc*. 2017;317(6):615–625. doi:10.1001/jama.2016.21040
10. Voelker R. What Is Allergic Rhinitis? *JAMA-J Am Med Assoc*. 2024;332(19):1682. doi:10.1001/jama.2024.14237
11. Wang X, Zhang H, Wang Y, et al. DNA sensing via the cGAS/STING pathway activates the immunoproteasome and adaptive T-cell immunity. *EMBO j*. 2023;42(8):e110597. doi:10.15252/embj.2022110597
12. Wheatley LM, Togias A. Clinical practice. allergic rhinitis. *New Engl J Med*. 2015;372(5):456–463. doi:10.1056/NEJMcp1412282
13. Cavagnero KJ, Badrani JH, Naji LH, et al. Cyclic-di-GMP induces STING-dependent ILC2 to ILC1 shift during innate type 2 lung inflammation. *Front Immunol*. 2021;12(null):618807. doi:10.3389/fimmu.2021.618807
14. Messaoud-Nacer Y, Culerier E, Rose S, et al. STING-dependent induction of neutrophilic asthma exacerbation in response to house dust mite. *Allergy*. 2024;null(null):null.
15. Midoro-Horiuti T, Goldblum R, Kuzume K, et al. Bisphenol A (BPA) has transgenerational effects on the development of experimental asthma through BRD4/ZDHHC-1/STING axis. *J Allergy Clin Immun*. 2023;151(2):Ab119. doi:10.1016/j.jaci.2022.12.376

16. Gruenwald A, Neururer M, Eidenhammer S, et al. The cGAS-STING pathway drives inflammation in Usual Interstitial Pneumonia, phagocytosis could prevent inflammation but is inhibited by the don't eat me signal CD47. *Pathol Res Pract*. 2024;260(null):155432. doi:10.1016/j.prp.2024.155432
17. Mdkhana B, Saheb Sharif-Askari N, Cagliani R, et al. Inhibiting DNA sensing pathway controls steroid hyporesponsive lung inflammation. *Adv Biol*. 2025;9(1):e2400230. doi:10.1002/adbi.202400230
18. Messaoud-Nacer Y, Culerier E, Rose S, et al. STING-dependent induction of neutrophilic asthma exacerbation in response to house dust mite. *Allergy*. 2025;80(3):715–737. doi:10.1111/all.16369
19. Schuliga M, Read J, Blokland KEC, et al. Self DNA perpetuates IPF lung fibroblast senescence in a cGAS-dependent manner. *Clin sci*. 2020;134(7):889–905. doi:10.1042/CS20191160
20. Tian M, Li F, Pei H, et al. The role of the cGAS-STING pathway in chronic pulmonary inflammatory diseases. *Front Med Lausanne*. 2024;11(null):1436091. doi:10.3389/fmed.2024.1436091
21. She L, Barrera GD, Yan L, et al. STING activation in alveolar macrophages and group 2 innate lymphoid cells suppresses IL-33-driven type 2 immunopathology. *JCI Insight*. 2021;6(3):null. doi:10.1172/jci.insight.143509
22. Wang H, Hu DQ, Xiao Q, et al. Defective STING expression potentiates IL-13 signaling in epithelial cells in eosinophilic chronic rhinosinusitis with nasal polyps. *J Allergy Clin Immun*. 2021;147(5):1692–1703. doi:10.1016/j.jaci.2020.12.623
23. Ahmad T, Kadam P, Bhiyani G, et al. Artemisia pallens W. Attenuates inflammation and oxidative stress in freund's complete adjuvant-induced rheumatoid arthritis in Wistar rats. *Diseases*. 2024;12(10):null. doi:10.3390/diseases12100230
24. Cheng C, Ho E, Chu K, et al. Anti-malarial drug artesunate attenuates allergic airway inflammation in A murine asthma model (140.18). *J immunol*. 2009;182(1_Supple):140–148. doi:10.4049/jimmunol.182.Supp.140.18
25. Cheng C, Ho WE, Goh FY, et al. Anti-malarial drug artesunate attenuates experimental allergic asthma via inhibition of the phosphoinositide 3-kinase/Akt pathway. *PLoS One*. 2011;6(6):e20932. doi:10.1371/journal.pone.0020932
26. Cheng C, Ng DS, Chan TK, et al. Anti-allergic action of anti-malarial drug artesunate in experimental mast cell-mediated anaphylactic models. *Allergy*. 2013;68(2):195–203. doi:10.1111/all.12077
27. Efferth T, Oesch F. The immunosuppressive activity of artemisinin-type drugs towards inflammatory and autoimmune diseases. *Med Res Rev*. 2021;41(6):3023–3061. doi:10.1002/med.21842
28. Nordmann T, Borrmann S, Ramharter M. Drug-induced hypersensitivity to artemisinin-based therapies for malaria. *Trends Parasitol*. 2022;38(2):136–146. doi:10.1016/j.pt.2021.08.011
29. Ravindra KC, Ho WE, Cheng C, et al. Untargeted proteomics and systems-based mechanistic investigation of artesunate in human bronchial epithelial cells. *Chem Res Toxicol*. 2015;28(10):1903–1913. doi:10.1021/acs.chemrestox.5b00105
30. Tan SS, Ong B, Cheng C, et al. The antimalarial drug artesunate inhibits primary human cultured airway smooth muscle cell proliferation. *Am J Resp Cell Mol*. 2014;50(2):451–458. doi:10.1165/rcmb.2013-0273OC
31. Wang Y, Wang A, Zhang M, et al. Artesunate attenuates airway resistance in vivo and relaxes airway smooth muscle cells in vitro via bitter taste receptor-dependent calcium signalling. *Exp Physiol*. 2019;104(2):231–243. doi:10.1113/EP086824
32. Li B, Zhang Z, Fu Y. Anti-inflammatory effects of artesunate on atherosclerosis via miR-16-5p and TXNIP regulation of the NLRP3 inflammasome. *Ann Transl Med*. 2021;9(20):1558. doi:10.21037/atm-21-4939
33. Wang Z, Feng X, Zhang G, et al. Artesunate ameliorates ligature-induced periodontitis by attenuating NLRP3 inflammasome-mediated osteoclastogenesis and enhancing osteogenic differentiation. *Int Immunopharmacol*. 2023;123(null):110749. doi:10.1016/j.intimp.2023.110749
34. Xie B, Li S, Bai W, et al. Artesunate alleviates hyperoxia-induced lung injury in neonatal mice by inhibiting NLRP3 inflammasome activation. *Evid-Based Complementary Altern Med*. 2023;2023(null):7603943. doi:10.1155/2023/7603943
35. Wei M, Xie X, Chu X, et al. Dihydroartemisinin suppresses ovalbumin-induced airway inflammation in a mouse allergic asthma model. *Immunopharm Immunot*. 2013;35(3):382–389. doi:10.3109/08923973.2013.785559
36. Zhang J, Li Y, Wan J, et al. Artesunate: a review of its therapeutic insights in respiratory diseases. *Phytomedicine*. 2022;104(null):154259. doi:10.1016/j.phymed.2022.154259
37. Zhang M, Lin J, Zhang J, et al. Artesunate inhibits airway remodeling in asthma via the MAPK signaling pathway. *Front Pharmacol*. 2023;14(null):1145188. doi:10.3389/fphar.2023.1145188